CONTRIBUTION FROM THE DEPARTMENT OF CHEMISTRY,
PRINCETON UNIVERSITY, PRINCETON, NEW JERSEY 08540

Raman and Infrared Spectra of Tetrameric Thallium(I) Alkoxides and Their Analysis[1a]

BY VICTOR A. MARONI[1b] AND THOMAS G. SPIRO

Received June 13, 1967

Raman and infrared spectra are reported for $Tl_4(OR)_4$ (R = ethyl and *n*-propyl). The bands are assigned on the basis of the tetrahedral structure known for thallium methoxide. A normal coordinate analysis was carried out for the $Tl_4(OC)_4$ core of the alkoxides. As in the case of $Pb_4(OH)_4^{4+}$,[2] agreement with the observed frequencies was readily obtained, but only if a direct interaction between metal atoms was included in the force field. Again the high intensity of the lowest frequency Raman bands provides evidence in favor of metal–metal bonding. The bonding scheme proposed for $Pb_4(OH)_4^{4+}$ is also applicable here. In the series $Tl_4(OR)_4$, $Pb_4(OH)_4^{4+}$, and $Bi_6(OH)_{12}^{6+}$ the calculated metal–metal stretching force constants are 0.26, 0.54, and 0.95 mdyn/Å. Evidently the strength of the proposed metal–metal bonds varies directly with nuclear charge.

Introduction

The previous two papers[2,3] described vibrational analyses for polynuclear hydroxy complexes of the isoelectronic cations Bi(III) and Pb(II). A major conclusion was that the low-frequency Raman spectra of these species could best be interpreted on the assumption of weak metal–metal bonding.

The third cation in this isoelectronic series is Tl(I). Thallous ion interacts only weakly with hydroxide, apparently by ion pairing, since there is no Raman evidence for Tl–OH binding in aqueous solution.[4] However thallous alkoxides are tetrameric in organic solvents, as first shown by the molecular weight determinations of Sidgwick and Sutton.[5] These authors suggested that the thallium atoms might be arranged tetrahedrally, and this was confirmed for crystalline $Tl_4(OCH_3)_4$ by Dahl, *et al.*[6]

The Tl_4O_4 unit in thallium alkoxides is isoelectronic with the Pb_4O_4 unit in $Pb_4(OH)_4^{4+}$, and evidently it is also isostructural. In fact the Tl–Tl separation, 3.83 Å, determined by Dahl *et al.*, is only 0.02 Å larger than the Pb–Pb distance in $Pb_4(OH)_4^{4+}$.[2] Although the positions of the methoxy groups in $Tl_4(OCH_3)_4$ could not be determined, Dahl, *et al.*, suggested that they were most likely located above the tetrahedral faces, as are the hydroxyl groups in $Pb_4(OH)_4^{4+}$.

We report here the Raman and infrared spectra of liquid thallium ethoxide, $Tl_4(OC_2H_5)_4$, together with a vibrational analysis, based on the assumption that the tetrahedral arrangement found in the methoxide is retained in the ethoxide. The low-frequency Raman and infrared spectra of solid thallous *n*-propoxide are also reported and they lend support to the assumption that substitution of one alkyl group for another does not significantly influence the central Tl_4O_4 unit. Attempts to obtain the Raman spectrum of thallous methoxide were unsuccessful, owing to its instability, especially under the influence of the mercury arc radiation of the Raman spectrophotometer. The isopropoxide proved similarly unstable.

Except for complications introduced by the ethyl groups, the vibrational spectrum of $Tl_4(OC_2H_5)_4$ is analogous to that of $Pb_4(OH)_4^{4+}$,[2] and the results of the vibrational analysis are quite similar. In particular metal–metal bonds are again implicated, although they seem to be only half as strong for Tl(I) as for Pb(II).

Experimental Section

The thallous alkoxides were prepared as described in the literature.[5] The liquid ethoxide was filtered through a fine frit in a nitrogen atmosphere. Spectra were run immediately to avoid decomposition. As prepared, the ethoxide has a small amount of ethanol dissolved in it, and decomposition was much less rapid if the ethanol was not removed. The solid *n*-propoxide was dried over sodium *in vacuo* for several hours before its spectra were taken.

Raman spectra were recorded at a sample temperature of 28 ± 1° with a Cary Model 81 Raman spectrophotometer using the 4358-Å mercury line for excitation. A standard 7-mm liquid cell was used for the ethoxide, and a conical solid cell[7] was used for the *n*-propoxide. Polarization measurements were made on the ethoxide using polaroid cylinders surrounding the sample tube. All attempts to obtain Raman spectra of thallous methoxide or isopropoxide failed owing to rapid decomposition of the samples.

Infrared spectra were recorded from 180 to 650 cm^{-1} with a Beckman IR-12 spectrophotometer. Samples were mulled in Nujol and pressed between $^1/_{16}$-in. polyethylene windows. A nitrogen purge was maintained in the sample compartment during all measurements.

Results and Assignments

There are numerous Raman frequencies of thallous ethoxide above 500 cm^{-1}, which arise from vibrations of the ethoxide group. These are listed in Table I along with tentative assignments based on Krishman's[8] assignments of corresponding lines in the spectrum of ethanol. The Raman spectrum below 500 cm^{-1} is shown in Figure 1a, while that of thallous *n*-

(1) (a) This investigation was supported by Public Health Service Grant GM-13498, from the National Institute of General Medical Sciences; (b) NASA Predoctoral Fellow.

(2) V. A. Maroni and T. G. Spiro, *Inorg. Chem.*, **7**, 188 (1968).

(3) V. A. Maroni and T. G. Spiro, *ibid.*, **7**, 183 (1968).

(4) J. H. B. George, J. A. Rolfe, and L. A. Woodward, *Trans. Faraday Soc.*, **49**, 375 (1953).

(5) N. V. Sidgwick and L. E. Sutton, *J. Chem. Soc.*, 1461 (1930).

(6) L. F. Dahl, G. L. Davis, D. L. Wampler, and R. West, *J. Inorg. Nucl. Chem.*, **24**, 357 (1962).

(7) R. H. Busey and O. L. Keller, *J. Chem. Phys.*, **41**, 215 (1964).

(8) K. Krishman, *Proc. Indian Acad. Sci., Sect. A*, **53**, 151 (1961).

TABLE I

$Tl_4(OC_2H_5)_4$ RAMAN BANDS ABOVE 500 CM^{-1} [a]

Frequency, cm^{-1}	Intensity[b]	Polarization	Assignment
798	4	dp	CH_2 rock
878	7	dp	C–C str
1047	3	dp	C–O str
1098	11	p	CH_2 twist
1148	3	dp	CH_3 wag
1282	3	dp	CH_2 wag
1355	9	p	C–H bend
1374	7	p	C–H bend
1444	12	p	C–H bend
1472	7	p	C–H bend
2586	8	?	C–H str
2686	17	?	C–H str
2729	7	?	C–H str
2800	100	p	C–H str
2820	13	?	C–H str
2854	36	p	C–H str
2904	60	p	C–H str
2914	19	?	C–H str
2949	47	?	C–H str

[a] Symbols: p, polarized; dp, depolarized; ?, polarization uncertain. [b] The intensity of the 63-cm^{-1} band shown in Figure 1a is 81 relative to 100 for the 2800-cm^{-1} band.

propoxide is shown in Figure 1b. The latter decomposed appreciably during the spectral determination and all features above 300 cm^{-1} were obscured. The infrared spectra of the alkoxides are shown in Figure 2.

We note at once the presence in both Raman spectra of three strong low-frequency bands, at 102, 63, and 44 cm^{-1} (the last is obscured by the exciting line for the *n*-propoxide). The highest of the three is polarized in the ethoxide spectrum, and therefore is of A_1 symmetry, while the others are depolarized. Their frequencies are in the ratios 2:1.24:0.86, not far from the theoretical ratios, $2:\sqrt{2}:1$, expected for the A_1, F_2, and E modes of a tetrahedral array of like atoms, assuming a single force constant.[2] The inference is therefore strong that we are indeed dealing with a tetrahedral cage structure.

If we consider only the central $Tl_4(OC)_4$ portion of the thallous alkoxides, then for a tetrahedral structure the representation of the Raman- and infrared-active vibrations is $\Gamma_{vib} = 3A_1 + 3E + 5F_2$. All of the modes are Raman active and the F_2 modes are active in the infrared as well. One A_1 and one F_2 mode are expected to arise from symmetric and antisymmetric stretching of the O–C bonds and should lie at high frequencies. Since there is no reason to expect much C–O stretch–stretch interaction across the cage, these vibrations are both assigned to the 1047-cm^{-1} Raman frequency, listed in Table I. The remaining vibrations are expected to lie at much lower frequencies.

The three lowest frequency Raman modes are assigned to the A_1, F_2, and E vibrations of the Tl_4 cage, as discussed in the preceding paragraph. We are then left with six bands, expected somewhat above 100 cm^{-1}. A broad band appears at ~290 cm^{-1} in the Raman spectrum of the ethoxide and in the infrared spectra of both alkoxides and can be assigned to an F_2 mode. However, the Raman band is partially polarized, and it

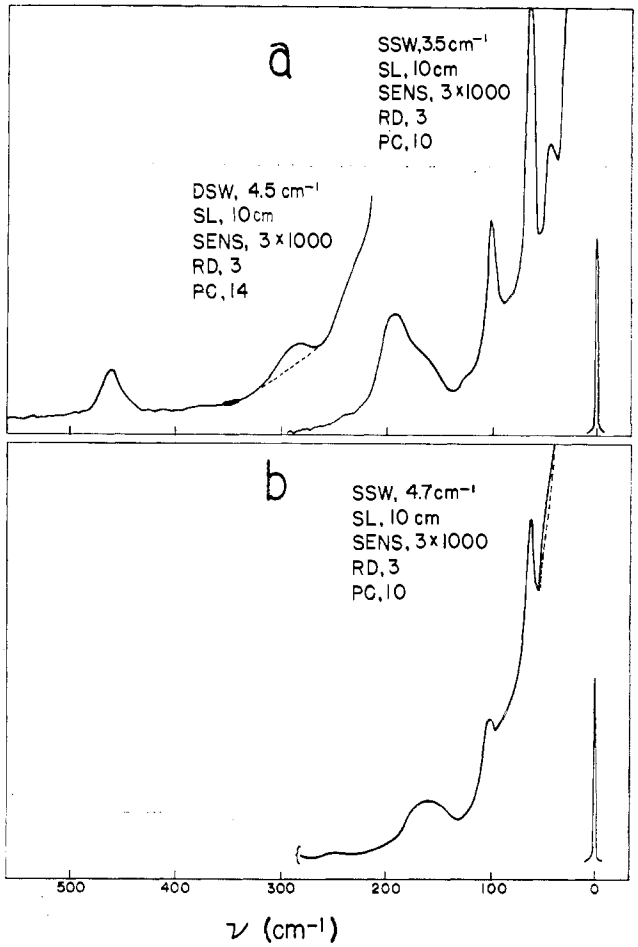

Figure 1.—Raman spectra of (a) thallous ethoxide (liquid) and (b) thallous *n*-propoxide (crystalline solid), using a Cary Model 81 and scan speed of 0.25 cm^{-1}/sec. Abbreviations: SSW = single slit width; SL = slit length; PC = period control; SENS = sensitivity setting; RD = Raman dymode setting.

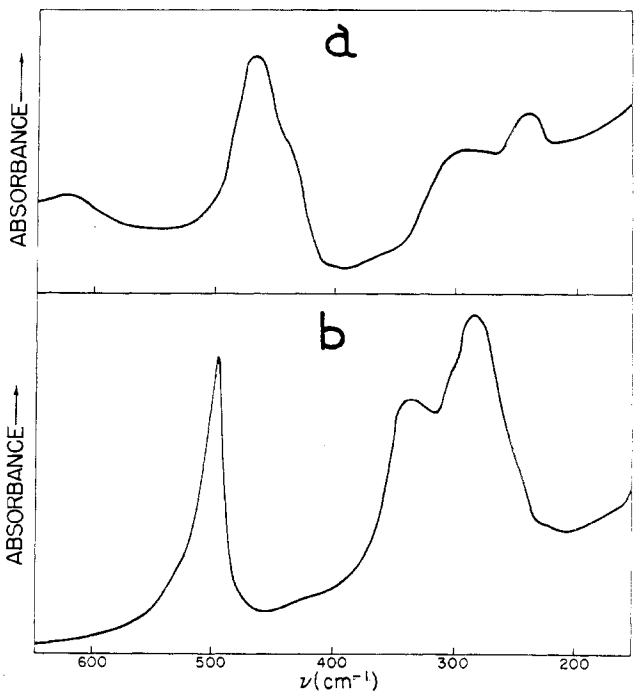

Figure 2.—Infrared spectra of (a) thallous ethoxide and (b) thallous *n*-propoxide, in Nujol mull using a Beckman IR-12; double beam; gain 6%; slit program standard.

therefore appears to contain the third A_1 mode (symmetric Tl–O stretching) as well. Another F_2 mode can be assigned to 462 cm^{-1}, where a band is observed in both the Raman and the infrared spectra of the ethoxide and in the infrared spectrum of the *n*-propoxide (shifted here to 490 cm^{-1}).

The remaining assignments are based on the normal coordinate analysis, described in the next section. It appears that the 462-cm^{-1} band contains an E mode as well as an F_2 mode, and that the broad 165-cm^{-1} band, observed in both Raman spectra (the frequency is below the available infrared range), also contains an E and an F_2 mode. There remains an unexplained band at 195 cm^{-1} in the ethoxide Raman spectrum. It is absent in the *n*-propoxide spectrum and is probably not a genuine mode of the $Tl_4(OC)_4$ cage. It might arise from a hindered rotational mode in the ethoxide groups. The infrared spectra show additional absorptions, at 620 and 430 cm^{-1} for the ethoxide, and at 330 cm^{-1} for the isopropoxide. Similar bands appear in the spectra of the corresponding alcohols.

Normal Coordinate Analysis

An analysis was carried out for the vibrations of the tetrahedral $Tl_4(OC)_4$ unit, the assignments for which are discussed above. The approximation involved in isolating this unit is that its vibrations do not mix significantly with those of the hydrogen atoms and the methyl groups. For the cage modes below 500 cm^{-1}, with which we are primarily concerned, this approximation should be quite good.

F and *G* matrices were constructed according to Wilson, Decius, and Cross.[9] The Tl–Tl distance was taken as that found for thallous methoxide,[6] 3.83 Å. The Tl–O distance was taken as 2.57 Å, the Pb–O distance in $Pb_4(OH)_4^{4+}$,[2] and a distance of 1.43 Å was assumed for the C–O bond.[10] The internal coordinates are defined in Figure 3.

As in the analysis for $Pb_4(OH)_4^{4+}$,[2] it was found that a force field based exclusively on metal–oxygen stretching and bending coordinates (in addition here to carbon–oxygen coordinates) was unsuccessful in reproducing the observed frequencies with a limited number of reasonable force constants. Again, when the metal–oxygen bending coordinates (angles α and β) were replaced by a metal–metal interaction, an excellent fit was obtained with a minimum number of force constants. The symmetry coordinates used are given in Table II. Table III lists the contributions of the internal coordinates and the redundancy conditions in each symmetry class. The force constants are defined in Table IV which also lists the *F* matrix elements formed from them. Calculation of the *G* matrix elements and solution of the secular equation with least-squares refinement of the force constants were carried out by computer, using programs SD-4064 and SD-4032, both due to Schachtschneider.[11] The results are shown under calculation I in Table V. Clearly an entirely adequate fit to the data is obtained with only four valence force constants. (The F_2 mode calculated at 142 cm^{-1} appears discrepant, but the observed 165-cm^{-1} band is quite broad, *cf.* Figure 1b, and could well contain a component near this frequency.) The potential energy distribution from this calculation is given in Table VI. The stretching coordinates are well separated in the various normal modes, but C–O–Tl bending contributes substantially to most of the low-frequency modes. Thus, while the 102-cm^{-1} A_1 mode is

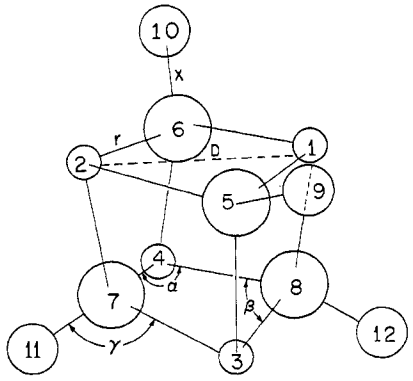

Figure 3.—Arrangement of thallium atoms (smallest circles), oxygen atoms (largest circles), and carbon atoms (medium circles) in the model assumed for $Tl_4(OR)_4$. Parameters: r = 2.57 Å, X = 1.43 Å, D = 3.83 Å, α = 84°, β = 96°, γ = 123°.

TABLE II
SYMMETRY COORDINATES FOR $Tl_4(OC)_4$[a]

A_1

$$S_X^{(A_1)} = \frac{1}{2}[X(5,9) + X(6,10) + X(7,11) + X(8,12)]$$

$$S_\gamma^{(A_1)} = \frac{1}{\sqrt{12}}[\gamma(1,5,9) + \gamma(2,5,9) + \gamma(3,5,9) + \gamma(1,6,10) + \gamma(2,6,10) + \gamma(4,6,10) + \gamma(2,7,11) + \gamma(3,7,11) + \gamma(4,7,11) + \gamma(1,8,12) + \gamma(3,8,12) + \gamma(4,8,12)]$$

E

$$S_X^{(E)} = 0\ (X \text{ does not contribute to E})$$

$$S_\gamma^{E} = \frac{1}{\sqrt{24}}[2\gamma(1,6,10) + 2\gamma(2,5,9) + 2\gamma(3,7,11) + 2\gamma(4,8,12) - \gamma(1,5,9) - \gamma(1,8,12) - \gamma(2,6,10) - \gamma(2,7,11) - \gamma(3,5,9) - \gamma(3,8,12) - \gamma(4,7,11) - \gamma(4,6,10)]$$

F_2

$$S_X^{(F_2)} = \frac{1}{\sqrt{12}}[3X(5,9) - X(6,10) - X(7,11) - X(8,12)]$$

$$S_{\gamma(1)}^{(F_2)} = \frac{1}{\sqrt{12}}[\gamma(1,5,9) + \gamma(2,5,9) + \gamma(3,5,9) + \gamma(4,7,11) + \gamma(4,6,10) + \gamma(4,8,12) - \gamma(1,6,10) - \gamma(2,6,10) - \gamma(2,7,11) - \gamma(3,7,11) - \gamma(1,8,12) - \gamma(3,8,12)]$$

$$S_{\gamma(2)}^{(F_2)} = \frac{1}{\sqrt{6}}[\gamma(1,5,9) + \gamma(2,5,9) + \gamma(3,5,9) - \gamma(4,6,10) - \gamma(4,7,11) - \gamma(4,8,12)]$$

[a] The symmetry coordinates for the metal–oxygen bonds, r, and the metal–metal bonds, D, are the same as those given for $Pb_4(OH)_4^{4+}$ in Table II of the previous paper.[2] Symbols: r, X, γ, D = internal coordinates defined in Figure 3. Numbers in parentheses refer to atoms connected by the internal coordinates, following the numbering system in Figure 3.

(9) E. B. Wilson, J. C. Decius, and P. C. Cross, "Molecular Vibrations," McGraw-Hill Book Co., Inc., New York, N. Y., 1955.
(10) H. M. M. Shearer and C. B. Spencer, *Chem. Commun.*, 194 (1966).
(11) R. G. Snyder and J. H. Schachtschneider, *Spectrochim. Acta*, **19**, 117 (1963).

TABLE III

CONTRIBUTIONS OF THE INTERNAL COORDINATES TO THE NORMAL MODES FOR $Tl_4(OC)_4$

Internal coordinate	Number of contributions to each symmetry class		
	A_1	E	F_2
r	1	1	2
X	1	0	1
γ	1	1	2
D	1	1	1

Redundancy conditions

A_1

$$-1.0545S_r^{(A1)} + 1.5998S_\gamma^{(A1)} + S_D^{(A1)} = 0$$

F_2

$$-0.4661S_{r(1)}^{(F2)} - 0.6592S_{r(2)}^{(F2)} + 0.4419S_D^{(F2)} + 0.7071S_{\gamma(1)}^{(F2)} + S_{\gamma(2)}^{(F2)} = 0$$

TABLE IV

NONZERO SYMMETRY F MATRIX ELEMENTS FOR $Tl_4(OC)_4$[a]

A_1

$F_{rr} = K_r$
$F_{xx} = K_x$
$F_{\gamma\gamma} = H_\gamma$
$F_{DD} = D$

E

$F_{rr} = K_r$
$F_{\gamma\gamma} = H_\gamma$
$F_{DD} = D$

F_2

$F_{r(1)r(1)} = K_r$
$F_{r(2)r(2)} = K_r$
$F_{xx} = K_x$
$F_{\gamma(1)\gamma(1)} = H_\gamma$
$F_{\gamma(2)\gamma(2)} = H_\gamma$
$F_{DD} = D$

[a] Symbols: K_r = Tl–O stretching force constant, K_x = C–O stretching force constant, H_γ = bending constant at the angle γ, D = Tl–Tl interaction.

TABLE V

SUMMARY OF VIBRATIONAL CALCULATIONS FOR $Tl_4(OC)_4$

Species	Frequencies, cm^{-1}		
	Obsd	Calculation I	Calculation II
A_1	1047	1047	1047
	Ca. 290	287	301
	102	100	101
E	*Ca.* 462	462	448
	Ca. 165	158	172
	44	43	42
F_2	1047	1047	1047
	Ca. 462	469	452
	Ca. 290	282	303
	Ca. 165	151	162
	63	66	65
	Force constants, mydn/Å		
K_r		1.434	1.339
K_x		4.189	4.136
H_γ		0.068	0.084
D		0.270	0.257

primarily Tl–Tl stretching, it contains a 31% contribution from C–O–Tl bending.

Because the metal–oxygen distance is the least certain of the molecular parameters used, its influence was tested by lengthening it by 0.14 Å, as in the $Pb_4(OH)_4^{4+}$ analysis,[2] and repeating the calculation. The results are shown under Calculation II in Table V. There are slight readjustments in the force constants, and the discrepancies between calculated and observed frequencies for the 165- and 462-cm^{-1} bands are slightly outside experimental error. These discrepancies can be removed by inclusion of a small stretch–stretch interaction at the angle α.

TABLE VI

POTENTIAL ENERGY DISTRIBUTION FOR $Tl_4(OC)_4$

Normal mode frequency, cm^{-1}	V_{rr}[a]	V_{XX}	$V_{\gamma\gamma}$	V_{DD}
1047 (A_1)	6	94	0	0
1047 (F_2)	6	94	1	0
462 (E)	82	0	18	0
462 (F_2)	82	0	18	0
290 (A_1)	89	6	3	2
290 (F_2)	88	6	5	1
165 (E)	18	0	81	1
148 (F_2)	18	0	81	1
102 (A_1)	0	0	27	73
63 (F_2)	0	0	11	89
44 (E)	0	0	1	99

[a] $V_{i,j}$ = normalized contribution to the potential energy from F matrix elements of the type (i,j).

Discussion

The low-frequency vibrational spectra of thallous ethoxide and *n*-propoxide are in quantitative accord with a tetrahedral cage structure for these tetrameric species, on the assumption of reasonable molecular parameters. The least certain of these, the Tl–O distance, has little influence on the vibrational analysis. As in the case of $Pb_4(OH)_4^{4+}$,[2] the observed frequencies are inadequately reproduced, as long as the valence interactions are limited to metal–oxygen (and carbon–oxygen) bonds. Inclusion of a metal–metal interaction leads to a highly efficient fit of the data. All eleven frequencies (nine of them independently observed) are reproduced with only four force constants.

Again metal–oxygen and metal–metal stretching coordinates are well separated in the normal modes. However, C–O–Tl bending mixes significantly into several of the low-frequency modes. In the polynuclear Pb(II) and Bi(III) hydroxy complexes,[2,3] motions of the hydroxide hydrogen could be entirely neglected. For those complexes it was suggested that evidence for the reality of metal–metal bonds is provided by the high Raman intensity observed for the low-frequency cage modes. This argument applies here also, but it is of interest that among the three cage modes, the A_1 band is no longer the most intense, as it was for $Pb_4(OH)_4^{4+}$. Now the F_2 band is the most intense, while the A_1 band, though still quite strong, is substantially weaker. Part of this reversal may be accounted for by the mixing in of C–O–Tl bending. While this motion contributes only 11% to the potential energy of the F_2 mode, its contribution to the A_1 mode is 31%. Presumably the polarizability change involved in C–O–Tl bending is considerably less than that produced by motions of the Tl_4 cage.

A bonding scheme designed to take weak metal–metal bonding into account in the thallous alkoxides would be identical with that proposed[2] for $Pb_4(OH)_4^{4+}$. The thallium s and p_z orbitals could be allowed to hybridize and overlap in the Tl_4 cage to produce four bonding orbitals, accommodating the thallium valence electrons. The p_x and p_y orbitals would be available and appropriate for bonding to alkoxide. The resulting eight bonding orbitals would accommodate sixteen

alkoxide electrons, leaving one electron pair nonbonding on each oxygen. A suggested energy level scheme is shown in Figure 2 of ref 2. The average M–O bond order is still two-thirds, and the decrease in metal–oxygen stretching constant from 1.66 to 1.43 mdyn/Å, from $Pb_4(OH)_4^{4+}$ to $Tl_4(OR)_4$, presumably reflects the decrease in nuclear charge, although the change in ligand perhaps has an effect.

The bonding in thallium alkoxides has been considered by Kettle,[12] who placed it in an equivalent-orbital framework. In his view the Tl_4 tetrahedron should have associated with it four face-centered equivalent bonding orbitals, which can accommodate two σ electrons from each alkoxide oxygen. (This gives an average M–O bond order of one-third.) It should also have a set of six edge-centered bonding orbitals and a corresponding antibonding set. Twelve electrons on each thallium (5d as well as 6s) are included in the scheme, and six of them are set aside in nonbonding orbitals. The remaining six then fill up both the bonding and antibonding orbitals, and the conclusion from this scheme is that there is no net bonding between the thallium atoms. However the number of nonbonding orbitals used appears to be somewhat arbitrary, as indeed does the number of bonding orbitals. The crux of the matter lies in the total number of orbitals set aside for metal electrons. If it is just equal to the number already filled in the valence state of the isolated ions, then of course there will be no metal–metal bonding. For ions having $d^{10}s^2$ configuration, the valence p orbitals must be included if metal–metal bonds are to be invoked. In this series of articles[2,3] we have suggested a scheme for doing this. Whether it is in fact energetically feasible for the complexes under consideration remains to be determined.

An interesting result of the vibrational analysis is that the calculated metal–metal stretching constant increases by a factor of 2 (0.26 to 0.54 mdyn/Å) from $Tl_4(OR)_4$ to $Pb_4(OH)_4^{4+}$. On the other hand, the metal–metal distance is virtually identical for the two complexes. Any bonding scheme must reconcile these observations with the greater s–p energy gap for Pb(II) than for Tl(I). In the free ions the separation between the s^2 ground state and the lowest s^1p^1 excited state is 7.4 ev for Pb^{2+} and 6.1 ev for Tl^+.[13] If metal–metal bonds are stronger for Pb(II) than for Tl(I), the bonding orbitals of the former must be lowered relative to those of the latter by an amount more than sufficient to compensate for the increased s–p promotional energy. Such an effect might well result from the increase in nuclear charge on going from Tl(I) to Pb(II). The field produced by the greater charge would stabilize both localized s orbitals and bonding orbitals delocalized in the metal ion cage. The energy difference between the two would increase with increase in effective nuclear charge, on the basis of simple coulombic considerations. Consequently if the energy difference is favorable for metal–metal bonding in the case of Tl(I), it should be more so for Pb(II). This line of reasoning is strengthened by the observation that the metal–metal stretching constant is again nearly doubled (from 0.54 to 0.95 mdyn/Å) on going from $Pb_4(OH)_4^{4+}$ to $Bi_6(OH)_{12}^{6+}$. Here differences in structure and in metal–metal distance play a role, but the dominant effect is no doubt still the increase in nuclear charge.

Acknowledgments.—We are deeply indebted to Professor Niel Bartlett for stimulating discussions of our results in this entire series. This work made use of computer facilities supported in part by National Science Foundation Grant NSF GP 579.

(12) S. F. A. Kettle, *Theoret. Chim. Acta*, **4**, 150 (1966).

(13) C. E. Moore, "Atomic Energy Levels," Vol. III, Circular No 467, National Bureau of Standards, U. S. Government Printing Office, Washington, D. C., 1958.